Liquid Crystals
Publication details, including instructions for authors and subscription information:
http://www.informaworld.com/smpp/title~content=t713926090

Static and dynamic critical behaviours in de Vries liquid crystals

Yuji Sasaki[a]; Kenji Ema[a]; Haruhiko Yao[b]
[a] Department of Physics, Graduate School of Science and Engineering, Tokyo Institute of Technology, Tokyo, Japan [b] Department of Macromolecular Science and Engineering, Graduate School of Science and Technology, Kyoto Institute of Technology, Matsugasaki, Sakyo-ku, Kyoto, Japan

Online publication date: 28 May 2010

To cite this Article Sasaki, Yuji , Ema, Kenji and Yao, Haruhiko(2010) 'Static and dynamic critical behaviours in de Vries liquid crystals', Liquid Crystals, 37: 5, 571 — 577
To link to this Article: DOI: 10.1080/02678291003710458
URL: http://dx.doi.org/10.1080/02678291003710458

Liquid Crystals,
Vol. 37, No. 5, May 2010, 571–577

Taylor & Francis
Taylor & Francis Group

Static and dynamic critical behaviours in de Vries liquid crystals

Yuji Sasaki[a], Kenji Ema[a]* and Haruhiko Yao[b]

[a]*Department of Physics, Graduate School of Science and Engineering, Tokyo Institute of Technology, 2-12-1 Oh-okayama, Meguro, Tokyo 152-8550, Japan;* [b]*Department of Macromolecular Science and Engineering, Graduate School of Science and Technology, Kyoto Institute of Technology, Matsugasaki, Sakyo-ku, Kyoto 606-8585, Japan*

(*Received 22 December 2009; final version received 16 February 2010*)

Measurements of dielectric dispersion have been carried out on two liquid crystal compounds 8422[2F3] and 8O23[7F8-], showing non-layer-shrinkage (NLS) behaviour through the smectic-*A* (Sm-*A*)–smectic-*C* (Sm-*C*) transition. The critical exponent γ for the susceptibility determined from the data lies in the range 1.9–2.0 for 8422[2F3] and 1.1–1.2 for 8O23[7F8-]. While the former agrees with the general trend reported so far for this group of liquid crystals, the latter result is distinct from them, the γ value being definitely smaller. These observations indicate that the Sm-*A*–Sm-*C* transition with NLS behaviour can exhibit quasi two-dimensional Ising critical behaviour under certain conditions. The critical exponent Δ for the relaxation frequency has also been obtained as $\Delta = 2.0$–2.1 for 8422[2F3] and 1.2–1.3 for 8O23[7F8-]. The results support the general expectation $\Delta > \gamma$ rather than the conventional behaviour $\Delta = \gamma$.

Keywords: critical phenomena; dielectric dispersion; relaxation frequency; de Vries liquid crystals

1. Introduction

A group of liquid-crystalline compounds that has recently attracted much attention is characterised by almost non-layer-shrinkage (NLS) behaviour through the smectic-*A* (Sm-*A*)–smectic-*C* (Sm-*C*) transition, and that they also have unusually large electroclinic effects if the compound is chiral [1–6]. Since a structure suggested by de Vries *et al*. [7–9] has been accepted as one plausible explanation for the NLS behaviour, these compounds are often called de Vries liquid crystals. However, challenging questions regarding these compounds still remain to be answered.

Theoretically, it is expected that Sm-*A*–Sm-*C* phase transitions belong to the *XY* universality class [10]. Although experiments in the 1980s reported classical behaviours which can be described successfully with an extended Landau theory [11, 12], later it was found that the critical behaviours around the Sm-*A*–Sm-*C** transition exhibited by several liquid crystals showing antiferroelectricity can be well described with the three-dimensional (3D) *XY* critical exponents (see [13] and references therein).

Nevertheless, the situation has not been settled in the case of de Vries-type liquid crystals. Based on electrooptical measurements of the electroclinic response (see [14] and also a more recent and general report [15], and references therein), it has been found that the values of the critical exponent γ for several NLS-showing substances are definitely larger than the theoretical value for the 3D *XY* model, $\gamma = 1.316$ (see [16]). Here, γ is a critical exponent for the susceptibility χ, implying $\chi \propto |T - T_c|^{-\gamma}$ around the transition temperature T_c. Galli and co-researchers claimed that the transitions with NLS behaviour belong to a universality class different from the conventional Sm-*A*–Sm-*C* transitions [14]. Panarina *et al*. [17] predicted that $\gamma = 1.33$–2.0 for this type of transition. On the other hand, Krueger and Giesselmann [18] carried out dielectric spectroscopic measurements and reported a considerably broad mean-field regime, which seems to contradict the above observations.

Recently, the present authors undertook calorimetric and dielectric measurements [19] on liquid crystals showing NLS behaviour. It was revealed that heat capacity data for two of the studied substances, TSiKN65 as well as 8422[2F3], can be well fitted with a logarithmic divergence except in the immediate vicinity of the transition [19], in agreement with the expectation for the 2D Ising model [20]. It was also found that the critical exponent γ determined from the dielectric data for TSiKN65 lies at 1.8 ± 0.2, in agreement with the result by Selinger *et al*. obtained for the same compound from birefringence measurement [3], and again with the theoretical expectation for the 2D Ising value $\gamma = 1.75$ (see [21]). With all of these, further investigations in de Vries liquid crystals are required to establish a general and unified understanding of the phase transitions for

*Corresponding author. Email: kema@phys.titech.ac.jp

ISSN 0267-8292 print/ISSN 1366-5855 online

DOI: 10.1080/02678291003710458
http://www.informaworld.com

this group of liquid crystals. In connection with this, an important prospect lies in studying the dynamic critical behaviour. In particular, this is because the dynamic critical behaviour is closely related to the static behaviour (see, for instance, [23] and references therein), while detailed measurement of the dynamic properties from a viewpoint of the critical phenomena has seldom been reported on liquid crystals with the NLS behaviour.

In this article [22] we present the results of dielectric-dispersion measurements on 8422[2F3], together with 8O23[7F8-] which also exhibits the NLS behaviour through the Sm-*A**–Sm-*C** transition. The results for the two substances showed a marked contrast to each other. For 8422[2F3], γ was 1.9–2.0, which is close to the value for TSiKN65, and also the 2D Ising expectation. On the other hand, for 8O23[7F8-], a γ of 1.1–1.2 was found, which is in a marked contrast to the result for 8422[2F3] and other liquid crystals with the NLS behaviour. These results indicate that the Sm-*A*–Sm-*C* transition with NLS behaviour can exhibit quasi two-dimensional Ising critical behaviour under certain conditions. It has been pointed out that it is possible that two kinds of crossovers exist. The critical exponent Δ for the relaxation frequency has also been obtained. In particular, the results support the general expectation $\Delta > \gamma$ rather than the conventional behaviour $\Delta = \gamma$ (see [23]).

2. Experimental details

The molecular structures and phase sequences of the compounds studied in this work, 8422[2F3] and 8O23[7F8-], are shown in Figures 1(a) and (b), respectively. The values of the phase transition temperatures are based on the results of the calorimetric measurement made by the present authors [24].

(a) 8422[2F3]

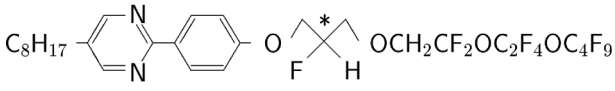

Isotropic (365.6K) Sm-*A* (339.1K) Sm-*C**

(b) 8O23[7F8-]

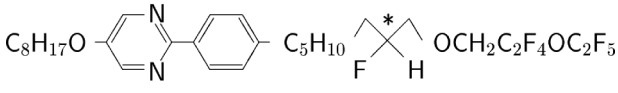

Isotropic (373.4K) Sm-*A* (357.4K) Sm-*C**

Figure 1. Molecular structures and phase sequences of (a) 8422[2F3] and (b) 8O23[7F8-].

Standard liquid crystal cells with thicknesses of 13.0 μm in 8422[2F3] and 14.8 μm in 8O23[7F8-] were used. The complex dielectric constant was measured over a frequency range of 150 Hz to 10 MHz with an HP 4192A impedance analyser. The amplitude of the ac signal applied to the sample cell was 0.1 V. Temperature was scanned with a rate of typically 0.005 K min^{-1} in 8422[2F3] and 0.01 K min^{-1} in 8O23[7F8-]. The data measured at each frequency were interpolated, and the frequency dependence of the complex dielectric constant was obtained.

3. Results and data analyses

3.1 Compound 8422[2F3]

Figure 2 shows a typical example of a Cole–Cole plot obtained for 8422[2F3]. Two dispersions are visible from the figure. One more dispersion was observed in the lower-frequency region, although it is not included in the figure. Among these three dispersions, the intermediate-frequency dispersion depends critically on temperature, and corresponds to the soft-mode dispersion. The other two do not show noticeable temperature dependence, and are ascribed to extrinsic origins. The low-frequency dispersion is thought to be mainly due to dc conductivity and/or surface effects. On the other hand, the high-frequency dispersion is presumably caused by insufficient conductivity of the indium tin oxide electrodes. In the present study we found that this effect can be approximated as a series connection of a resistance R_{ITO} to the sample with impedance $1/(i2\pi fC^*)$, where f is the measuring frequency, and C* represents the capacitance due to the complex dielectric constant ε* of the liquid crystal sample. In practice, the observed

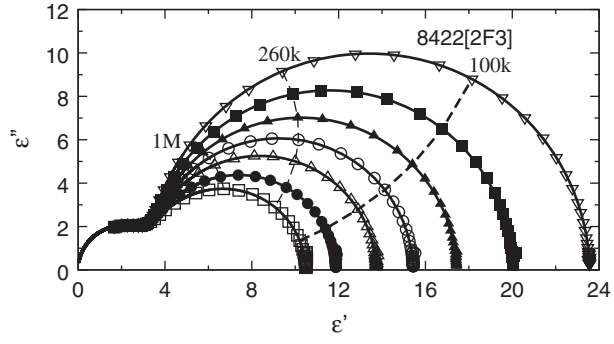

Figure 2. Typical Cole–Cole plots obtained from the dielectric measurement for 8422[2F3]. The solid lines are fitting curves based on Equations (1) and (2). Symbols represent data obtained at $T = 342.57$ K (□), 342.02 K (•), 341.46 K (Δ), 341.08 K (○), 340.72 K (▲), 340.35 K (■) and 339.98 K (▽).

'apparent' capacitance C^*_{obs} is related to the 'true' capacitance of the sample C^* as

$$\frac{1}{i2\pi f C^*_{obs}} = R_{ITO} + \frac{1}{i2\pi f C^*}, \quad (1)$$

and then the thus-obtained C^* is divided by a geometrical factor to obtain ε^*.

Assuming a standard Debye expression for the dispersion, the data have been fitted with

$$\varepsilon^* = \varepsilon_\infty + \frac{\Delta\varepsilon}{1 + [i(f/f_r)]^\beta} + g(f), \quad (2)$$

where f_r is the relaxation frequency, and $g(f)$ represents the lower-frequency contribution. The data were well fitted with this equation in most cases, as shown by solid lines in Figure 2. (Note that the data plotted in Figure 2 correspond to values before the correction of R_{ITO}, that is, the values of ε^*_{obs} obtained by dividing C^*_{obs} by a geometrical factor. The situation is the same in the results for 8O23[7F8-] described later.) The fact that the fitting is adequate is also seen from Figure 3, where typical frequency dependencies of the real part and the imaginary part of the complex dielectric constant are shown. The value of ε_∞ was around 4.0. The β value was very close to 1 for almost all temperatures

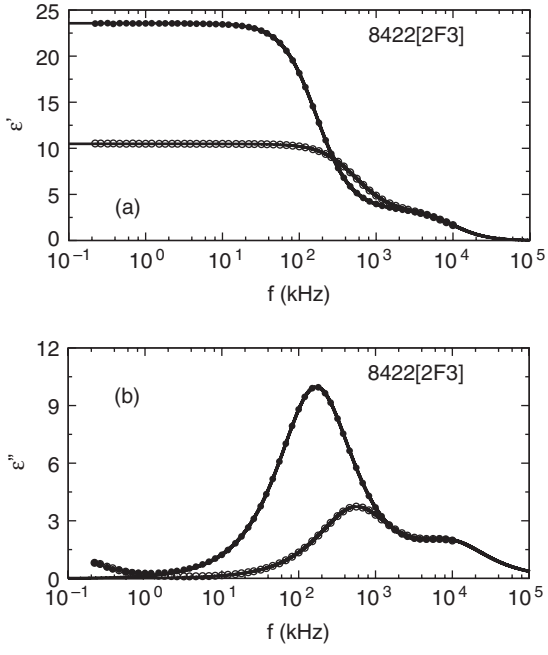

Figure 3. Typical frequency dependencies of (a) the real part and (b) the imaginary part of the complex dielectric constant obtained for 8422[2F3]. The solid lines are fitting curves based on Equations (1) and (2). Open circles represent data obtained at $T = 342.57$ K, and closed circles represent data obtained at $T = 339.98$ K.

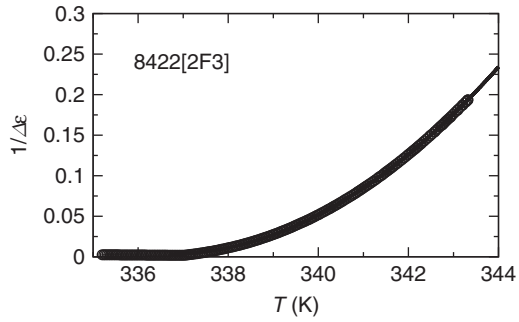

Figure 4. Temperature dependence of reciprocal of the relaxation strength $\Delta\varepsilon$ obtained for 8422[2F3]. The solid line is a fitting curve obtained using Equation (3) for data $0.003 < |t| < 0.02$ with $\gamma = 1.97$ and $T_c = 336.7$ K.

above T_c, showing the practically monodispersive nature of the relaxation.

The reciprocal of the relaxation strength $\Delta\varepsilon$ has been plotted against temperature in Figure 4. The data show a distinctly concave curve, indicating a deviation from the mean-field behaviour. In the present dielectric measurement, no sign of first-order nature was observed. The results for heating and cooling processes did not show any noticeable hysteresis, and no jump of the data suggesting a first-order transition was found. These features are the same as those observed in TSiKN65, and are understood to correspond to the very weak first-order nature of the transition.

The critical exponent γ has been determined from a fit to a power law

$$(\Delta\varepsilon)^{-1} = A|t|^\gamma + B. \quad (3)$$

The inclusion of the constant term B is justified in the existence of a surface layer with a low, temperature-independent dielectric constant, for example. We performed some measurements by applying an electric field. In the present analyses, however, we choose to use only data taken under zero field to avoid the effect of the field on the critical nature, which is not what we are interested in for the moment. The soft-mode dispersion is hidden by the Goldstone mode below T_c for the data under zero field, and therefore only data above T_c were used in the fit. To determine the T_c value, the temperatures giving the maximum of $\Delta\varepsilon$ and f_r under various values of field have been extrapolated to zero field, both yielding $T_c = 336.7$ K. This procedure is illustrated in Figure 5 for the case when $\Delta\varepsilon$ data are used, although an essentially identical result was obtained from the data for f_r. It is known that there is usually a narrow region in the immediate vicinity of the transition where observed data are affected by the impurities and/or instrumental resolutions. To avoid that the fits are affected by data points

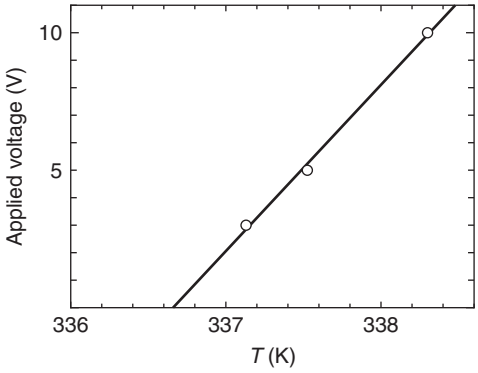

Figure 5. Procedure of determination of T_c. The temperatures of the maximum $\Delta\varepsilon$ observed for different bias field values have been extrapolated to zero field. Vertical axis shows the dc voltage applied across the sample cell.

Table 1. Fitting parameters and least-squares values obtained from fittings of the $\Delta\varepsilon$ data for 8422[2F3] to Equation (3). The unit for T_c is Kelvin. The parameters in brackets were held fixed at the value shown in the fits. The mean squared residual χ^2_ν has not been normalised.

$\lvert t\rvert_{max}$	T_c	γ	A	B	χ^2_ν
0.005	[336.7]	1.78	190.7	0.002	2.6×10^{-8}
0.01	[336.7]	1.82	230.4	0.002	2.7×10^{-8}
0.02	[336.7]	1.94	390.5	0.002	1.4×10^{-7}

in such a region, the data $T < 336.97$ K have not been used in the fit. The obtained parameter values are summarised in Table 1. Here, $|t|_{max}$ is the maximum value of the reduced temperature t used in the fit. Fits with smaller $|t|_{max}$ values yielded rather unstable results because of the one-sided fit as mentioned above, and also because the density of the data is much lower than the C_p data, and are not included in the table. It is seen that the γ value which gives the best fit in the χ^2_ν sense lies in the range 1.7–2.0.

It should be noted that the obtained γ value shows a tendency that it increases with the increase in $|t|_{max}$. On the other hand, it was found in our heat capacity measurement [19] that the heat anomaly showed an almost tricritical behaviour in the vicinity of the transition. It deserves attention that the decrease in γ observed in the present analyses for narrower data ranges is in a direction that approaches the value expected in the tricritical case, $\gamma = 1$. In the analyses of the heat capacity data [19], fits were tried excluding the data close to T_c, with $|t| < |t|_{min} = 0.003$. Hence, to be consistent with such fits, the present dielectric data were also fitted with the same constraint, and the results are shown in Table 2. We see that the result is more stable than in Table 1, and the most reliable

Table 2. Fitting parameters and least-squares values obtained from fittings of the $\Delta\varepsilon$ data for 8422[2F3] to Equation (3). The data close to T_c, with $|t| < |t|_{min} = 0.003$, have been excluded in the fits. The unit for T_c is Kelvin. The parameters in brackets were held fixed at the value shown in the fits. The mean squared residual χ^2_ν has not been normalised.

$\lvert t\rvert_{max}$	T_c	γ	A	B	χ^2_ν
0.01	[336.7]	1.89	310.5	0.003	3.1×10^{-9}
0.015	[336.7]	1.95	395.5	0.003	1.2×10^{-8}
0.02	[336.7]	1.97	431.7	0.003	2.2×10^{-8}
0.02	[336.7]	[1.75]	186.8	–0.003	4.4×10^{-6}
0.02	337.4	[1.75]	219.7	0.009	2.9×10^{-7}

value of γ seems to be 1.9–2.0. The solid line in Figure 4 shows the fitting curve with $\gamma = 1.97$ and $T_c = 336.7$ K for the case of $|t|_{max} = 0.02$. The fit seems adequate in this scale. Since the present result is close to that for TSiKN65, and the theoretical expectation for the 2D Ising model, $\gamma = 1.75$, fits were tried by fixing γ to 1.75, and the results are included in Table 2. With T_c still fixed at 336.7 K, the fit becomes slightly worse and with a negative B which seems unreasonable. Allowing T_c to be adjusted freely improves the fit quite acceptable in the χ^2_ν sense with a positive B.

Figure 6 shows the temperature dependence of the relaxation frequency f_r obtained for 8422[2F3]. The exponent Δ for the relaxation frequency has been determined by fitting the data with the following equation.

$$f_r = A_f |t|^{\Delta} + B_f \ . \tag{4}$$

In the same manner as in the fits for estimation of γ, two groups of fits were made. Table 3 shows results when all the data with $T > 336.97$ K have been used, while Table 4 shows those when the data with $|t| < |t|_{min} = 0.003$ have been excluded in the fits. It is

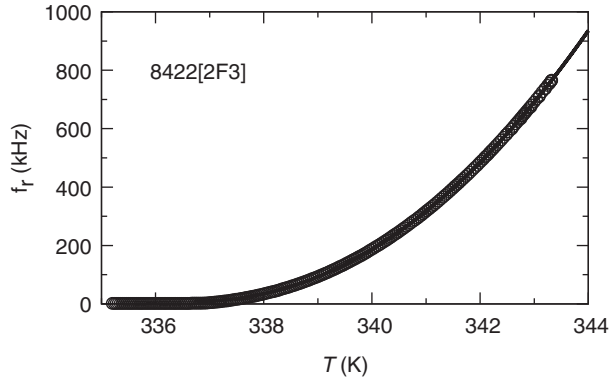

Figure 6. Temperature dependence of the relaxation frequency f_r obtained for 8422[2F3]. The solid line is a fitting curve obtained for data $0.003 < |t| < 0.02$ with $\Delta = 2.08$ and $T_c = 336.7$ K.

Table 3. Fitting parameters and least-squares values obtained from fittings of the relaxation frequency data for 8422[2F3] to Equation (4). The unit for T_c is Kelvin and for A_f and B_f is kilohertz. The parameters in brackets were held fixed at the value shown in the fits. The mean squared residual χ^2_ν has not been normalised.

$\|t\|_{max}$	T_c	Δ	$10^{-6} \times A_f$	B_f	χ^2_ν
0.005	[336.7]	1.76	0.57	1.9	2.5×10^{-2}
0.01	[336.7]	1.93	1.37	3.2	4.3×10^{-1}
0.02	[336.7]	2.06	2.44	6.0	2.0×10^{0}

Table 4. Fitting parameters and least-squares values obtained from fittings of the relaxation frequency data for 8422[2F3] to Equation (4). The data close to T_c, with $|t|<|t|_{min} = 0.003$, have been excluded in the fits. The unit for T_c is Kelvin and for A_f and B_f is kilohertz. The parameters in brackets were held fixed at the value shown in the fits. The mean squared residual χ^2_ν has not been normalised.

$\|t\|_{max}$	T_c	Δ	$10^{-6} \times A_f$	B_f	χ^2_ν
0.01	[336.7]	2.01	2.00	6.6	2.1×10^{-2}
0.015	[336.7]	2.06	2.49	8.4	1.2×10^{-1}
0.02	[336.7]	2.08	2.68	9.4	2.1×10^{-1}

seen that the results reveal a quite similar trend to the case for γ. When the data very close to T_c were included, the exponent Δ tends to increase for wider data ranges. With omitting the data in the vicinity of T_c, on the other hand, the Δ value is more stable, yielding $\Delta = 2.0$–2.1. From a comparison of the results in Tables 2 and 4, it is seen that the value of Δ is close to γ but clearly larger than γ, showing a non-conventional behaviour.

3.2 Compound 8O23[7F8-]

Figure 7 shows a typical Cole–Cole plot for 8O23[7F8-]. In comparison with the result for 8422[2F3], the main relaxation, responsible for the transition, appears in the lower-frequency region in the case of 8O23[7F8-]. Figure 8 shows typical frequency dependencies of the real part and the imaginary part of the complex dielectric constant. The value of ε_∞ was around 4.1. The relaxation strength $\Delta\varepsilon$ has been obtained using the same method as described above, and its reciprocals have been plotted against temperature in Figure 9. In contrast to the result for 8422[2F3], the data fall on an almost straight line indicating an almost mean-field behaviour.

Table 5 shows the values of the critical exponent γ and other parameters obtained from least-squares fits of the data to Equation (3). In these fits, T_c was fixed at

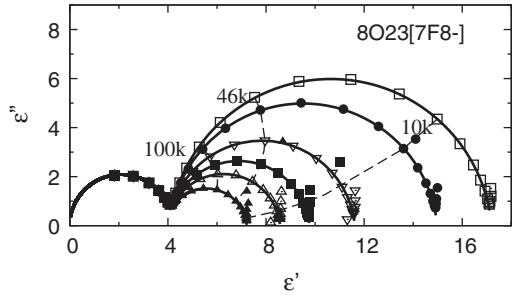

Figure 7. Typical Cole–Cole plots obtained from the dielectric measurement for 8O23[7F8-]. The solid lines are fitting curves based on Equations (1) and (2). Symbols represent data obtained at $T = 358.57$ K (▲), 358.17 K (Δ), 357.97 K (■), 357.77 K (▽), 357.58 K (•) and 357.51 K (□).

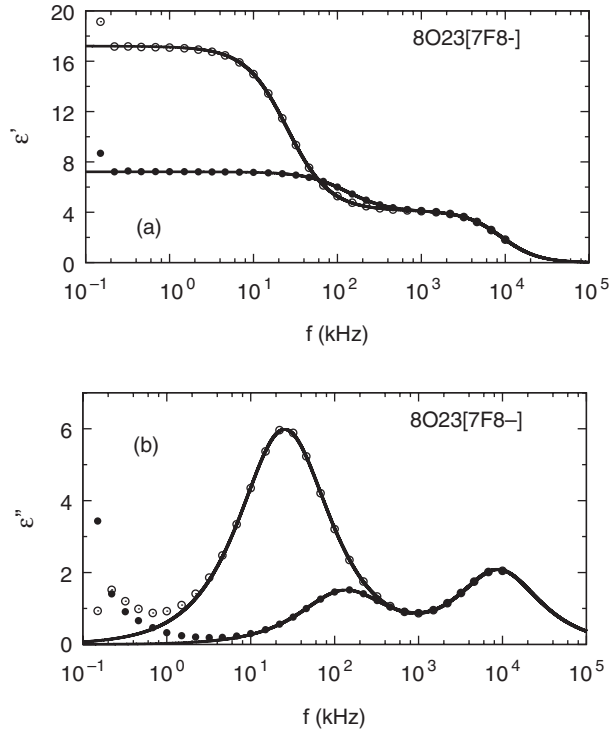

Figure 8. Typical frequency dependencies of (a) the real part and (b) the imaginary part of the complex dielectric constant obtained for 8O23[7F8-]. The solid lines are fitting curves based on Equation (1) and (2). Open circles represent data obtained at $T = 357.51$ K and closed circles represent data obtained at $T = 358.57$ K.

the temperature where $\Delta\varepsilon$ showed a maximum, $T_c = 357.1$ K. When γ was adjusted freely, the obtained value lies in the range $\gamma = 1.1$–1.2, which is stable for data-range shrinking. This value is definitely smaller than the 2D Ising value of 1.75. Fits were also tried with γ fixed at the 3D XY value 1.316, and the 3D Ising value 1.241, and the results have been included in the

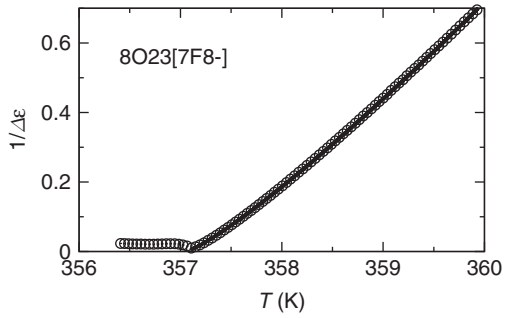

Figure 9. Temperature dependence of the reciprocal of the relaxation strength $\Delta\varepsilon$ obtained for 8O23[7F8-]. The solid line is a fitting curve obtained for the data range $|t|_{\max} = 0.005$ with $\gamma = 1.17$.

Table 5. Fitting parameters and least-squares values obtained from fittings of the $\Delta\varepsilon$ data for 8O23[7F8-] to Equation (3). The unit for T_c is Kelvin. The parameters in brackets were held fixed at the value shown in the fits. The mean squared residual χ^2_ν has not been normalised.

$\|t\|_{\max}$	T_c	γ	A	B	χ^2_ν
0.003	[357.1]	1.18	213.1	0.006	2.8×10^{-8}
0.003	[357.1]	[1.241]	295.8	0.010	9.1×10^{-7}
0.003	[357.1]	[1.316]	452.1	0.015	4.5×10^{-6}
0.005	[357.1]	1.17	201.4	0.006	4.5×10^{-8}
0.01	[357.1]	1.14	173.6	0.002	1.5×10^{-6}

table. It is seen that the fit clearly becomes worse by assuming such exponent values. Allowing T_c to be adjusted freely for the case $\gamma = 1.241$ gave a better fit in the χ^2_ν sense, $\chi^2_\nu = 9.9 \times 10^{-8}$ with $T_c = 356.97$ K, but B came out negative, $B = -0.012$.

Figure 10 shows the temperature dependence of the relaxation frequency f_r obtained for 8O23[7F8-]. The exponent Δ for the relaxation frequency has been determined in the same way as for 8422[2F3], and the results are shown in Table 6. The exponent value is

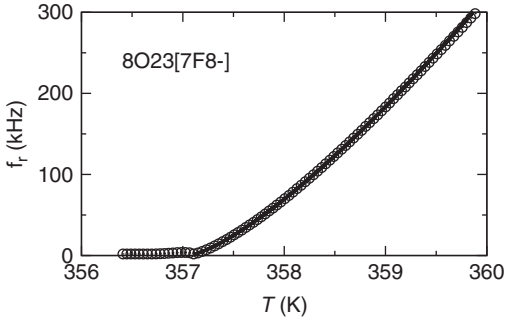

Figure 10. Temperature dependence of the relaxation frequency f_r obtained for 8O23[7F8-]. The solid line is a fitting curve obtained for the data range $|t|_{\max} = 0.005$ with $\Delta = 1.32$.

Table 6. Fitting parameters and least-squares values obtained from fittings of the relaxation frequency data for 8O23[7F8-] to Equation (4). The unit for T_c is Kelvin and for A_f and B_f is kilohertz. The parameters in brackets were held fixed at the value shown in the fits. The mean squared residual χ^2_ν has not been normalised.

$\|t\|_{\max}$	T_c	Δ	$10^{-6} \times A_f$	B_f	χ^2_ν
0.003	[357.1]	1.33	0.189	1.8	5.4×10^{-4}
0.005	[357.1]	1.32	0.184	1.7	4.9×10^{-3}
0.01	[357.1]	1.26	0.138	–1.1	1.0×10^{0}

stable against data-range shrinking, being $\Delta = 1.2$–1.3. Similarly to the result in 8422[2F3], it was also found here that $\Delta > \gamma$.

4. Discussion

The results of dielectric measurements carried out in the present work for two liquid crystals with the NLS behaviour are in remarkable contrast to each other. The γ value obtained for 8422[2F3], being 1.9–2.0, can be compared well with the value reported earlier for TSiKN65, and also close to the 2D Ising theoretical expectation, while it does not agree with the 3D XY value 1.316 (see [16]). It was found, on the other hand, that the γ value for 8O23[7F8-] is definitely smaller than the 2D Ising value. The value is still some way from the 3D XY expectation. Although it is relatively close to the 3D Ising value, the agreement seems marginal in the χ^2_ν sense. The deviation from the mean-field behaviour is distinct, the fit becomes clearly worse when $\gamma = 1$ is assumed.

To the best of the authors' knowledge, the present work is the first example where the dynamic behaviours have been studied quantitatively for de Vries liquid crystals. The critical exponent for the relaxation frequency, Δ, is determined as 2.0–2.1 for 8422[2F3] and 1.2–1.3 for 8O23[7F8-]. In particular, Δ is slightly but clearly larger than the susceptibility exponent γ in both cases, indicating the breakdown of the conventional theory which gives $\Delta = \gamma$ (see [23]). We also note here that the above value for 8422[2F3] almost agrees with the estimation $\Delta = 2.0$ for the 2D kinetic Ising model [25]. However, the difference between Δ and γ, being $\Delta - \gamma = 0.25$ in the theoretical expectation, seems wider than our present experimental result, $\Delta - \gamma \sim 0.1$.

Apparently, our present result for 8422[2F3] might seem to contradict that by Krueger and Giesselmann [18], since they reported a mean-field behaviour for the same substance. It should be noted, however, that the mean-field regime in their data lies at $|T - T_c| > 5$ K, as read from Figure 9 in [18]. Therefore, we see that the

present analyses have been made for the data closer to T_c than the mean-field regime. It is quite reasonable that the mean-field behaviour shown in a range far from T_c changes into a critical behaviour as it approaches T_c.

Experimental results reported so far have revealed that the γ values for substances showing de Vries behaviours are considerably higher than the 3D *XY* value 1.32, and, further, they have no particular value ranging from about 1.5–2.0 (see for instance [15]). Our result for 8422[2F3] and TSiKN65 agree with this trend. A natural scenario for explaining such wide spectrum of exponent values is that some kind of crossover occurs. We proposed to ascribe the critical behaviour for 8422[2F3] and also for TSiKN65 to the 2D Ising universality class. Although the reasoning presented there may be rather crude, it is still possible and seems reasonable that the general trend is a result of crossover from the 2D Ising to the 3D *XY* critical behaviours. One might be concerned that γ is higher than the 2D Ising value in some materials. A situation which deserves attention is the critical behaviour at nematic–smectic- *A* phase transitions, crossing over from 3D *XY* to tricritical behaviour [26]. It was reported that the observed γ rises *above* the *XY* value ($= 1.316$) before crossover toward tricriticality ($\gamma = 1$) occurs. This implies that the change in the critical exponent values during the crossover need not be monotonous in some cases.

As for the present result for 8O23[7F8], it does not fit in the general trend discussed above, and gives a new feature that γ is *below* the 3D *XY* value. The heat capacity anomaly of 8O23[7F8-] reported by the present authors in [24] shows a clearly asymmetric feature in contrast to the expectation for the 2D Ising behaviour. Although the data were fitted with the 3D *XY* model, a crossover behaviour to the tricritical behaviour was also found. Considering this, therefore, we recognise that the phase transition in this series of liquid crystals provides a notable situation which involves two kinds of crossovers.

After all, the critical behaviours of de Vries liquid crystals show various interesting and puzzling features. Theoretical studies are strongly desirable to understand them in a consistent manner, while much more effort should also be made from the experimental side.

Acknowledgements

The authors are grateful to Professor C.C. Huang and Professor H. Takezoe for helpful discussions, and Professor Y. Takanishi for technical help in the dielectric measurements. The liquid-crystal compounds were kindly provided by 3M Company, St Paul, Minnesota, USA. This work has been supported in part by the Global Center of Excellence Program by MEXT, Japan, through the Nanoscience and Quantum Physics Project of the Tokyo Institute of Technology.

References

[1] Giesselmann, F.; Zugenmaier, P; Dierking, I.; Lagerwall, S.T.; Stebler, B.; Kašpar, M.; Hamplová, V.; Glogarová, M. *Phys. Rev. E* **1999**, *60*, 598–602.
[2] Spector, M.S.; Heiney, P.A.; Naciri, J.; Weslowski, B.T.; Holt, D.B.; Shashidhar, R. *Phys. Rev. E* **2000**, *61*, 1579–1584.
[3] Selinger, J.V.; Collings, P.J.; Shashidhar, R. *Phys. Rev. E* **2001**, *64*, 061705-1–9.
[4] Clark, N.A.; Bellini, T.; Shao, R.F.; Coleman, D.; Bardon, S.; Link, D.R.; Maclennan, J.E.; Chen, X.H.; Wand, M.D.; Walba, D.M.; Rudquist, P.; Lagerwall, S.T. *Appl. Phys. Lett.* **2002**, *80*, 4097–4099.
[5] Lagerwall, J.P.F.; Giesselmann, F.; Radcliffe, M.D. *Phys. Rev. E* **2002**, *66*, 031703-1–11.
[6] Lagerwall, J.P.F.; Giesselmann, F. *ChemPhysChem* **2006**, *7*, 20–45.
[7] De Vries, A. *Mol. Cryst. Liq. Cryst.* **1977**, *41*, 27–31.
[8] De Vries, A.; Ekachai, A.; Spielberg, N. *Mol. Cryst. Liq. Cryst.* **1979**, *49* (L), 143–152.
[9] De Vries, A. *Mol. Cryst. Liq. Cryst.* **1979**, *49* (L), 179.
[10] De Gennes, P.G. *Mol. Cryst. Liq. Cryst.* **1973**, *21*, 49.
[11] Huang, C.C.; Viner, J.M. *Phys. Rev. A* **1982**, *25*, 3385–3388.
[12] Birgeneau, R.J.; Garland, C.W.; Kortan, A.R.; Litster, J.D.; Meichle, M.; Ocko, B.M.; Rosenblatt, C.; Yu, L.J.; Goodby, J. *Phys. Rev. A* **1983**, *27*, 1251–1254.
[13] Ema, K.; Yao, H. *Phys. Rev. E* **1998**, *57*, 6677–6684.
[14] Galli, G.; Reihmann, M.; Crudeli, A.; Chiellini, E.; Panarin, Yu.; Vij, J.; Blanc, C.; Lorman, V.; Olsson, N. *Mol. Cryst. Liq. Cryst.* **2005**, *439*, 245–257.
[15] Sandhya, K.L.; Panarin, Yu.P.; Panov, V.P.; Vij, J.K.; Dabrowski, R. *Eur. Phys. J. E* **2008**, *27*, 397–405.
[16] Bagnuls, C.; Bervillier, C. *Phys. Rev. B* **1985**, *32*, 7209–7231.
[17] Panarina, O.E.; Panarin, Yu.P.; Vij, J.K.; Spector, M.S.; Shashidhar, R. *Phys. Rev. E* **2003**, *67*, 051709.
[18] Krueger, M.; Giesselmann, F. *Phys. Rev. E* **2005**, *71*, 041704.
[19] Takekoshi, K.; Sasaki, Y.; Ema, K.; Yao, H.; Takanishi, Y.; Takezoe, H. *Phys. Rev. E* **2007**, *75*, 031704.
[20] Onsager, L. *Phys. Rev.* **1944**, *65*, 117–149.
[21] Fisher, M.E. *J. Math. Phys.* **1964**, *5*, 944–962.
[22] Ema, K.; Sasaki, Y.; Yao, H.; Huang, C.C. *Ferroelectrics* **2008**, *364*, 7–12.
[23] Hohenberg, P.C.; Halperin, B.I. *Rev. Mod. Phys.* **1977**, *49*, 435–479.
[24] Ema, K.; Takekoshi, K.; Yao, H.; Wang, S.T.; Huang, C.C. *Phys. Rev. E* **2005**, *71*, 031706.
[25] Yahata, H.; Suzuki, M. *J. Phys. Soc. Jpn.* **1969**, *27*, 1421.
[26] Garland, C.W.; Nounesis, G. *Phys. Rev. E* **1994**, *49*, 2964–2971.